Supplemental information

Quantitative study of unsaturated transport of glycerol through aquaglyceroporin that has high affinity for glycerol

Roberto A. Rodriguez[1], Ruth Chan[1], Huiyun Liang[1,2], and Liao Y. Chen[1*]

[1]Department of Physics, The University of Texas at San Antonio, San Antonio, Texas 78249 USA

[2]Department of Pharmacology, The University of Texas Health Science Center at San Antonio, San Antonio, Texas 78229 USA

The supplemental information (SI) contains three parts. In Part I, we provide four additional figures that are discussed but not included in the main text. In Part II, we give the long formulas and a figure for saturated *vs*. unsaturated transport flux. In Part III, we give alternative fittings to the experimental data.

Part I.

Fig. S1 illustrates the all-atom model of an AQP3 tetramer embedded in a patch of lipid bilayers mimicking the lipid compositions of the inner and the outer leaflets of human erythrocyte membrane.

Fig. S2 to S4 show the experimental data along with the theoretical curves for glycerol uptake at ~5°C, ~16°C, and ~37°C respectively.

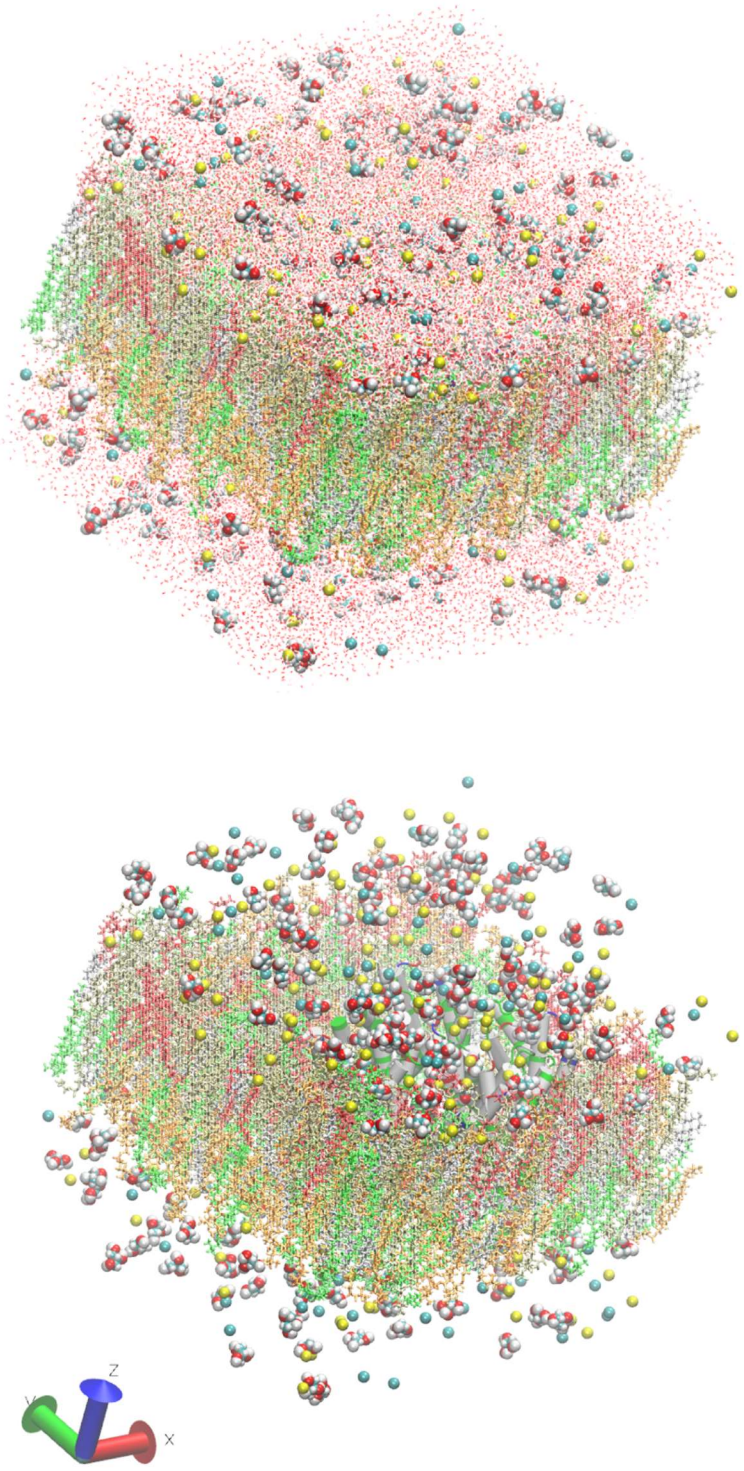

Fig. S1. All-atom model system of an AQP3 tetramer in a membrane patch mimicking the lipid composition of the human erythrocyte membrane. The system consists of 156,137 atoms. The intracellular space is located at $z > 20$Å and the extracellular space at $z < -20$Å. The water molecules are shown in the top panel as red-and-white dots but not shown in the bottom panel for a clearer view of all the other constituents of the system. The glycerol molecules and salt (NaCl) are shown as spheres colored by atom names (C, cyan; O, red; N, blue; H, white; Cl, cyan; K, metallic; Na, yellow). The lipids are represented as licorices colored lipid names (POPC, orange; POPE, tan; POPS, red; SSM, green; CHL, silver). The proteins are presented as surfaces colored by residue types (hydrophilic, green; hydrophobic, white; positively charged, blue; negatively charged, red). Molecular graphics in this paper were rendered with VMD[1].

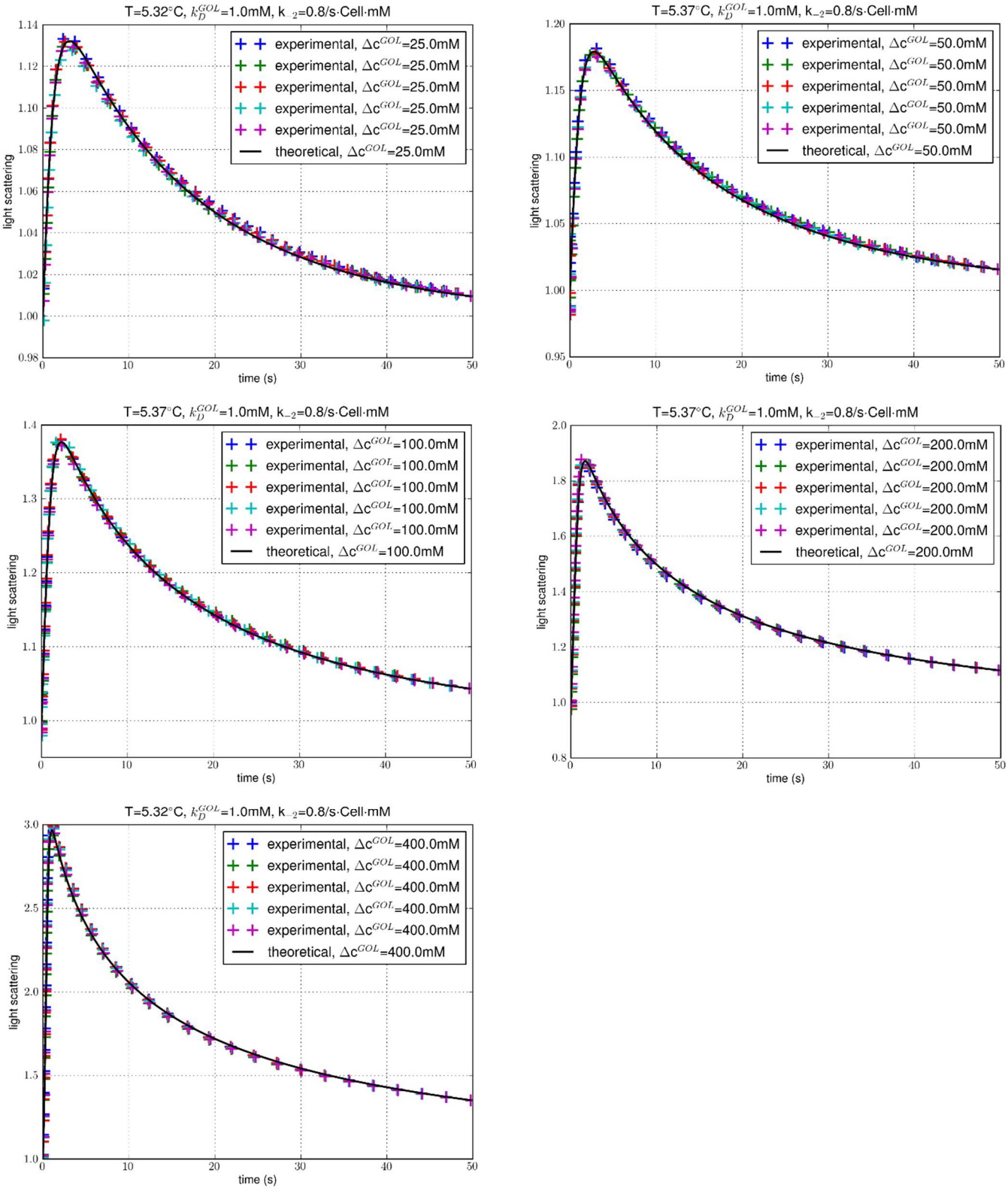

Fig. S2. Experiments at ~5°C of glycerol uptake into human erythrocytes for extracellular glycerol concentration at 25 mM, 50 mM, 100 mM, 200 mM, and 400 mM. The data points (colored crosses) represent normalized intensity of light scattered at 90° immediately after mixing of an erythrocyte suspension in 0.7 ×PBS (containing no glycerol) with an equal volume of 0.7 ×PBS containing $2 \times \Delta c^{GOL}$ glycerol. Five colors represent five experimental repeats under identical conditions. The black solid curve is the predicated time course with a single fitting parameter k_{-2}whose fitted values are shown. The fitting has a p-value less than 10^{-5} in all five sets and a relative error ~5%.

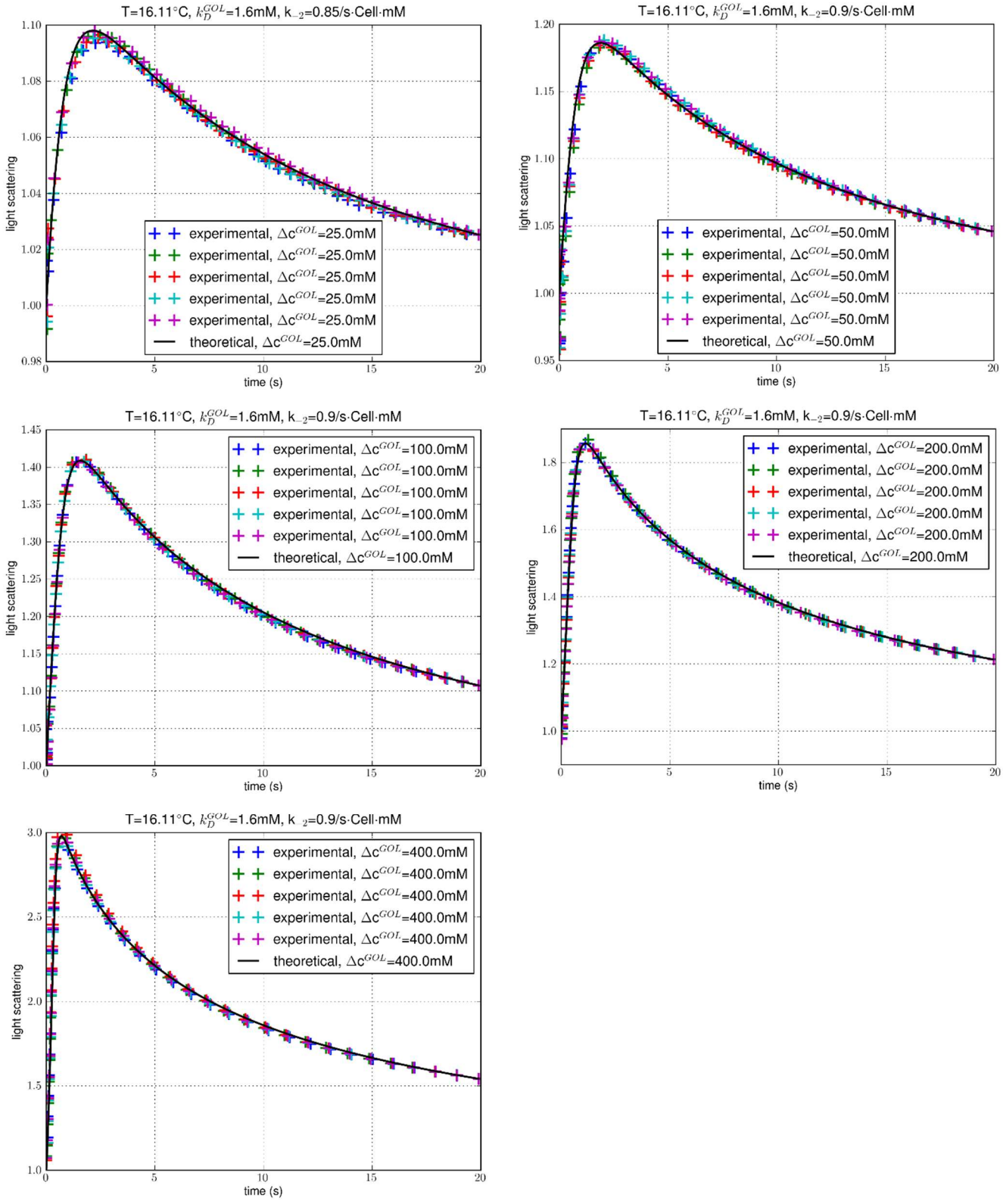

Fig. S3. Experiments at ~16°C of glycerol uptake into human erythrocytes for extracellular glycerol concentration at 25 mM, 50 mM, 100 mM, 200 mM, and 400 mM. The data points (colored crosses) represent normalized intensity of light scattered at 90° immediately after mixing of an erythrocyte suspension in 0.7 ×PBS (containing no glycerol) with an equal volume of 0.7 ×PBS containing $2 \times \Delta c^{GOL}$ glycerol. Five colors represent five experimental repeats under identical conditions. The black solid curve is the predicated time course with a single fitting parameter k_{-2}whose fitted values are shown. The fitting has a p-value less than 10^{-5} in all five sets and a relative error ~5%.

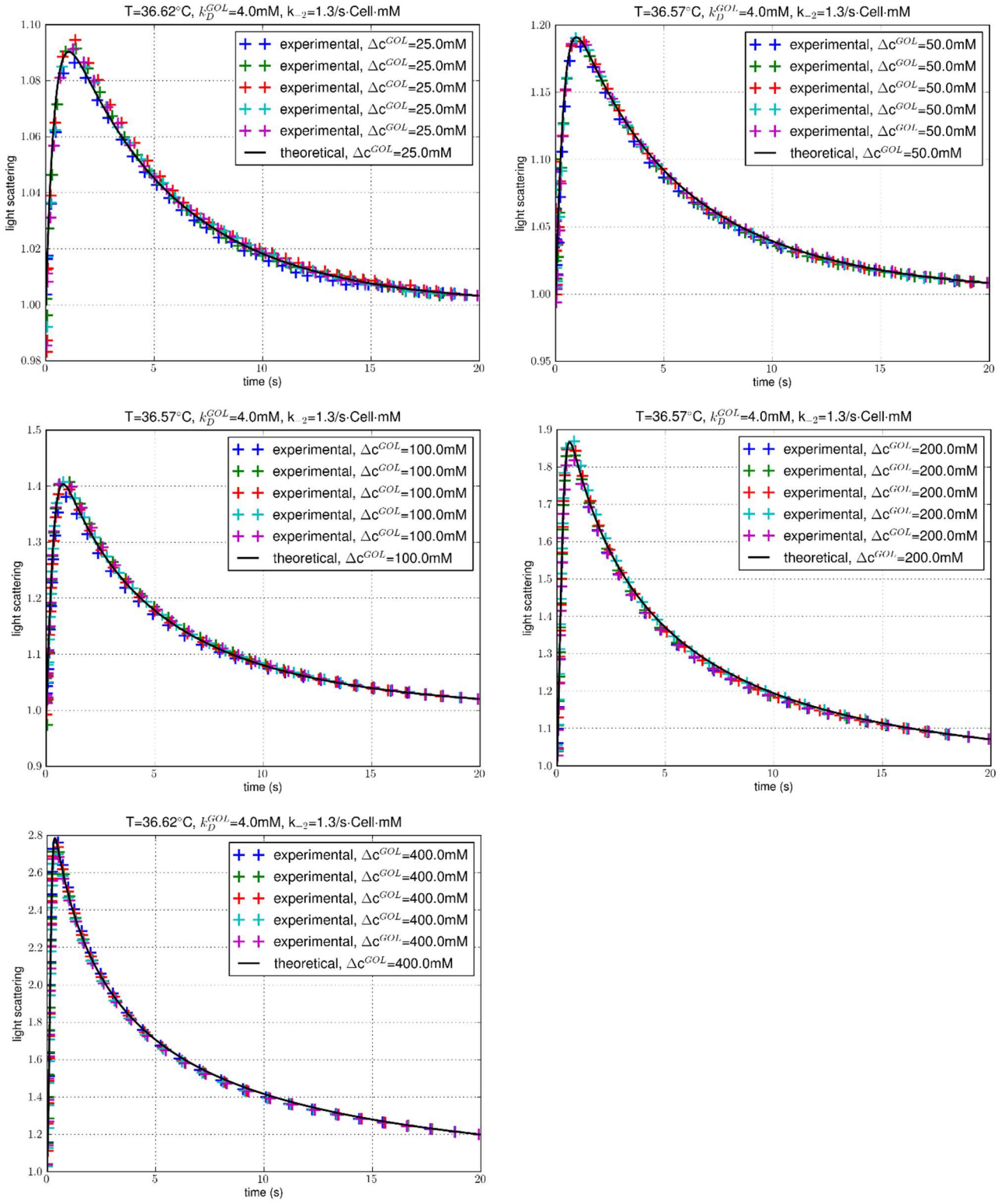

Fig. S4. Experiments at ~37°C of glycerol uptake into human erythrocytes for extracellular glycerol concentration at 25 mM, 50 mM, 100 mM, 200 mM, and 400 mM. The data points (colored crosses) represent normalized intensity of light scattered at 90° immediately after mixing of an erythrocyte suspension in 0.7 ×PBS (containing no glycerol) with an equal volume of 0.7 ×PBS containing $2 \times \Delta c^{GOL}$ glycerol. Five colors represent five experimental repeats under identical conditions. The black solid curve is the predicated time course with a single fitting parameter k_{-2}whose fitted values are shown. The fitting has a p-value less than 10^{-5} in all five sets and a relative error ~5%.

Part II.

The probabilities for the eight states are governed by the following equations of transport kinetics:

$$
\begin{aligned}
\frac{dp_{000}}{dt} &= k_1\, k_{D1}\, p_{100} + k_{-2}\, k_{D2}\, p_{001} - (k_1\, c_1 + k_{-2}\, c_2)\, p_{000},\\
\frac{dp_{100}}{dt} &= k_1\, c_1\, p_{000} - k_1\, k_{D1}\, p_{100} + k\,\frac{k_D}{k_{D1}}\, p_{010} - k\, p_{100},\\
\frac{dp_{010}}{dt} &= k\, p_{100} + k\, p_{001} + k_1\, k_{D1}\, p_{110} + k_{-2}\, k_{D2}\, p_{011} - \left(\frac{k\, k_D}{k_{D1}} + \frac{k\, k_D}{k_{D2}}\right) p_{010} - (k_1\, c_1 + k_{-2}\, c_2)\, p_{010},\\
\frac{dp_{001}}{dt} &= k_{-2} c_2 p_{000} - k_{-2}\, k_{D2}\, p_{001} + k\,\frac{k_D}{k_{D2}}\, p_{010} - k\, p_{001},\\
\frac{dp_{110}}{dt} &= k_1\, c_1\, p_{010} + k_{-2}\, k_{D2}\, p_{111} + k\, p_{011} + k\, p_{101} - (k\,\frac{k_{D1}}{k_{D2}} + k_1\, k_{D1} + k_{-2}\, c_2 + k\,\frac{k_D}{k_{D2}})\, p_{110},\\
\frac{dp_{011}}{dt} &= k_{-2}\, c_2\, p_{010} + k_1\, k_{D1}\, p_{111} + k\,\frac{k_{D1}}{k_{D2}}\, p_{110} + k\, p_{101} - \left(k + k_1\, c_1 + k_{-2}\, k_{D2} + k\,\frac{k_D}{k_{D1}}\right) p_{011},\\
\frac{dp_{111}}{dt} &= k_{-2}\, c_2\, p_{110} + k_1\, c_1\, p_{011} - (k_1\, k_{D1} + k_{-2}\, k_{D2})\, p_{111},\\
\frac{dp_{101}}{dt} &= k_{-2}\, c_2\, p_{100} + k_1\, c_1\, p_{001} - \left(k_1\, k_{D1} + k_{-2}\, k_{D2} + k\,\frac{k_D}{k_{D1}} + k\,\frac{k_D}{k_{D2}}\right) p_{101}.
\end{aligned}
\tag{1}
$$

Here the rate constants are tabulated in Table II for the transitions illustrated in Fig. 3A of the main text. It can be verified that these probabilies are normalizable:

$$p_{000} + p_{100} + p_{010} + p_{001} + p_{011} + p_{110} + p_{111} + p_{101} = 1. \tag{2}$$

The flux going into the IC side and the flux leaving the EC side are, respectively,

$$
\begin{aligned}
J_2 &= k_{-2}\, k_{D2}\, (p_{001} + p_{011} + p_{101} + p_{111}) - k_{-2}\, c_2 (p_{000} + p_{010} + p_{110} + p_{100}),\\
J_1 &= k_1\, c_1 (p_{011} + p_{010} + p_{001} + p_{000}) - k_1\, k_{D1}\, (p_{110} + p_{111} + p_{101} + p_{100}).
\end{aligned}
\tag{3}
$$

Under the quasi-stationary conditions, we found $J = J_2 = J_1 = K(c_e - c)$ with the EC concentration noted as $c_1 = c_e$ and the IC concentration $c_2 = c$. The flux is a rather complex function of the concentrations in the following equation (4). Illustrated in Fig. S5 is the flux J as a function of the EC concentration c_e when the IC concentration $c = 0$ at 23°C (yellow curve) in contrast with the case when the transitions between State 110 and State 011 were ignored (blue curve).

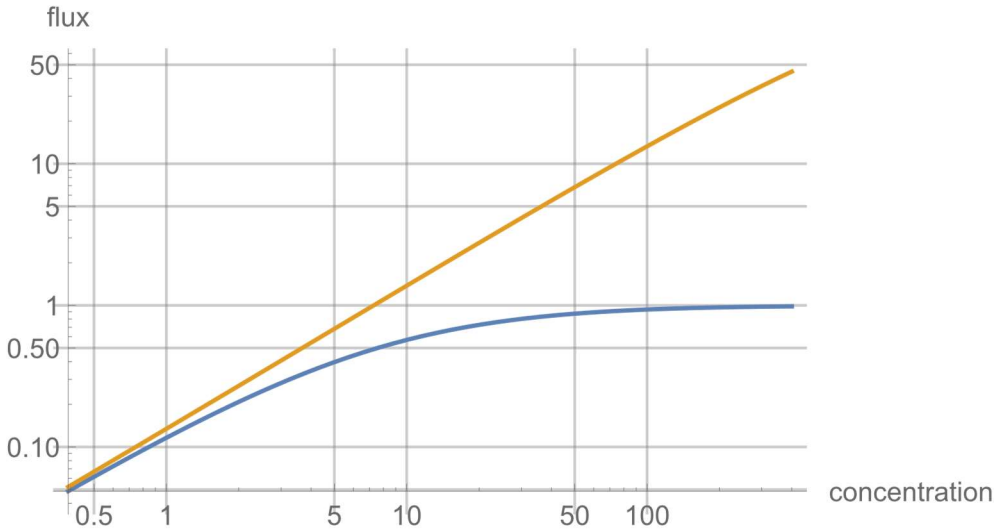

Fig. S5. J [1/s] *vs.* c_e [mM]. The curves show unsaturated characteristics (yellow) *vs.* saturated characteristics (blue) if the transitions between State 011 and State 110 were not included.

$$
\begin{aligned}
J = (c_e - c)(&k\mathrm{k_1k_{-2}k_{D1}k_{D2}}(\mathrm{c^2k_{-2}^2}\,(\mathrm{k_D + 2k_{D1}})(k + \mathrm{k_1k_{D1}}) + \mathrm{c_e^2k_1^2}(\mathrm{k_D + 2k_{D1}})(k + \mathrm{k_{-2}k_{D2}}) + \mathrm{k_D}(\mathrm{k_1k_{D1}} \\
&+ \mathrm{k_{-2}k_{D2}})(k(\mathrm{k_1 + k_{-2}})(\mathrm{k_D + 2k_{D1}}) + 2\mathrm{k_1k_{-2}k_{D1}k_{D2}}) \\
&+ \mathrm{c_e k_1}\big(k(\mathrm{k_D + 2k_{D1}})(\mathrm{k_1k_{D1}} + \mathrm{k_{-2}k_{D2}}) + \mathrm{c\,k_{-2}}(\mathrm{k_D + 2k_{D1}})(2k + \mathrm{k_1k_{D1}} + \mathrm{k_{-2}k_{D2}}) \\
&+ \mathrm{k_{-2}k_{D2}}(\mathrm{k_1k_{D1}}(3\mathrm{k_D} + 2\mathrm{k_{D1}}) + \mathrm{k_{-2}}(\mathrm{k_D + 2k_{D1}})\mathrm{k_{D2}})\big) \\
&+ \mathrm{c\,k_{-2}}(k(\mathrm{k_D + 2k_{D1}})(\mathrm{k_1k_{D1}} + \mathrm{k_{-2}k_{D2}}) + \mathrm{k_1k_{D1}}(\mathrm{k_1\,k_{D1}}(\mathrm{k_D + 2k_{D1}}) \\
&+ \mathrm{k_{-2}}(3\mathrm{k_D} + 2\mathrm{k_{D1}})\mathrm{k_{D2}})))) / (\mathrm{c^3k_{-2}^3}(\mathrm{k_D + 2k_{D1}})(k + \mathrm{k_1k_{D1}})^2\mathrm{k_{D2}} \\
&+ \mathrm{k_Dk_{D1}k_{D2}}(\mathrm{k_1k_{D1}} + \mathrm{k_{-2}k_{D2}})(k(\mathrm{k_1 + k_{-2}})(\mathrm{k_D + 2k_{D1}}) + 2\mathrm{k_1k_{-2}k_{D1}k_{D2}})(k(\mathrm{k_1 + k_{-2}}) \\
&+ \mathrm{k_1k_{-2}}(\mathrm{k_{D1} + k_{D2}})) + \mathrm{c_e^3k_1^3k_{D1}}(k + \mathrm{k_{-2}k_{D2}})(k(\mathrm{k_D + 2k_{D1}}) + \mathrm{k_{-2}k_{D2}}(2\mathrm{c} + \mathrm{k_D} + 2\mathrm{k_{D2}})) \\
&+ \mathrm{c^2k_{-2}^2}(k + \mathrm{k_1k_{D1}})\Big(k(\mathrm{k_D + 2k_{D1}})(\mathrm{k_D} + \mathrm{k_{D1}} + \mathrm{k_{D2}})(\mathrm{k_1k_{D1}} + \mathrm{k_{-2}k_{D2}}) \\
&+ \mathrm{k_1k_{D1}k_{D2}}\big(\mathrm{k_1k_{D1}}(\mathrm{k_D + 2k_{D1}}) + \mathrm{k_{-2}}(2\mathrm{k_Dk_{D1}} + 3\mathrm{k_Dk_{D2}} + 4\mathrm{k_{D1}k_{D2}})\big)\Big) \\
&+ \mathrm{ck_{-2}}(k^2(\mathrm{k_1 + k_{-2}})(\mathrm{k_D + 2k_{D1}})\big(\mathrm{k_{1k_{D1}} + k_{-2}k_{D2}}\big)\big(\mathrm{k_{D1}k_{D2}} + \mathrm{k_D}(\mathrm{k_{D1} + k_{D2}})\big) \\
&+ 2\mathrm{k_1}^2\,\mathrm{k_{-2}}\,\mathrm{k_{D1}}^2\mathrm{k_{D2}}\Big(\mathrm{k_1}\,\mathrm{k_{D1}}\big(\mathrm{k_{D1}k_{D2}} + \mathrm{k_D}(\mathrm{k_{D1} + k_{D2}})\big) \\
&+ \mathrm{k_{-2}k_{D2}}\big(\mathrm{k_{D1}k_{D2}} + 2\mathrm{k_D}(\mathrm{k_{D1} + k_{D2}})\big)\Big) \\
&+ k\mathrm{k_1k_{D1}}(\mathrm{k_1}^2\,\mathrm{k_{D1}}(\mathrm{k_D + 2k_{D1}})\big(\mathrm{k_{D1}k_{D2}} + \mathrm{k_D}(\mathrm{k_{D1} + k_{D2}})\big) + \mathrm{k_{-2}}^2\,\mathrm{k_{D2}}(\mathrm{k_D}^2\,(\mathrm{k_{D1} + k_{D2}}) \\
&+ 2\mathrm{k_{D1}k_{D2}}(\mathrm{k_{D1} + k_{D2}}) + \mathrm{k_D}(2\mathrm{k_{D1}}^2 + 7\mathrm{k_{D1}k_{D2}} + 2\mathrm{k_{D2}}^2)) + \mathrm{k_1k_{-2}}(\mathrm{k_D^2}(\mathrm{k_{D1} + k_{D2}})^2 \\
&+ 2\mathrm{k_{D1}^2k_{D2}}(\mathrm{k_{D1} + 2k_{D2}}) + \mathrm{k_Dk_{D1}}(2\mathrm{k_{D1}^2} + 7\mathrm{k_{D1}k_{D2}} + 7\mathrm{k_{D2}^2}))) \\
&+ \mathrm{c_e^2k_1^2}\Big(2\mathrm{c^2k_{-2}^2k_{D1}k_{D2}}(2k + \mathrm{k_1k_{D1}} + \mathrm{k_{-2}k_{D2}}) \\
&+ (k + \mathrm{k_{-2}k_{D2}})\Big(k(\mathrm{k_D + 2k_{D1}})(\mathrm{k_D} + \mathrm{k_{D1}} + \mathrm{k_{D2}})(\mathrm{k_1k_{D1}} + \mathrm{k_{-2}k_{D2}}) \\
&+ \mathrm{k_{-2}k_{D1}k_{D2}}\big(\mathrm{k_{-2}k_{D2}}(\mathrm{k_D + 2k_{D2}}) + \mathrm{k_1}(3\mathrm{k_Dk_{D1}} + 2\mathrm{k_Dk_{D2}} + 4\mathrm{k_{D1}k_{D2}})\big)\Big) \\
&+ \mathrm{ck_{-2}}\Big(k^2(\mathrm{k_D + 2k_{D1}})(2\mathrm{k_{D1}} + \mathrm{k_{D2}}) \\
&+ \mathrm{k_{-2}k_{D1}k_{D2}}\big(6\mathrm{k_1k_{D1}k_{D2}} + \mathrm{k_1k_D}(\mathrm{k_{D1} + k_{D2}}) + \mathrm{k_{-2}k_{D2}}(\mathrm{k_D} + 4\mathrm{k_{D2}})\big) \\
&+ k\Big(\mathrm{k_1k_{D1}}\big(\mathrm{k_D}(\mathrm{k_{D1} + k_{D2}}) + 2\mathrm{k_{D1}}(\mathrm{k_{D1}} + 2\mathrm{k_{D2}})\big) \\
&+ \mathrm{k_{-2}k_{D2}}\big(\mathrm{k_D}(3\mathrm{k_{D1}} + \mathrm{k_{D2}}) + 2\mathrm{k_{D1}}(\mathrm{k_{D1}} + 4\mathrm{k_{D2}})\big)\Big)\Big)\Big) + \mathrm{c_ek_1}(2\mathrm{c^3k_{-2}^3k_{D1}}(k + \mathrm{k_1k_{D1}})\mathrm{k_{D2}} \\
&+ k^2(\mathrm{k_1 + k_{-2}})(\mathrm{k_D + 2k_{D1}})(\mathrm{k_1k_{D1}} + \mathrm{k_{-2}k_{D2}})(\mathrm{k_{D1}k_{D2}} + \mathrm{k_D}(\mathrm{k_{D1} + k_{D2}})) \\
&+ 2\mathrm{k_1k_{-2}^2k_{D1}}\,\mathrm{k_{D2}}^2(\mathrm{k_{-2}k_{D2}}(\mathrm{k_{D1}k_{D2}} + \mathrm{k_D}(\mathrm{k_{D1} + k_{D2}})) + \mathrm{k_1k_{D1}}(\mathrm{k_{D1}k_{D2}} + 2\mathrm{k_D}(\mathrm{k_{D1} + k_{D2}}))) \\
&+ \mathrm{c^2k_{-2}^2}(k + \mathrm{k_1k_{D1}})(k(\mathrm{k_D + 2k_{D1}})(\mathrm{k_{D1} + 2k_{D2}}) + \mathrm{k_{D2}}(\mathrm{k_1k_{D1}}(\mathrm{k_D} + 4\mathrm{k_{D1}}) + 6\mathrm{k_{-2}k_{D1}k_{D2}} \\
&+ \mathrm{k_{-2}k_D}(\mathrm{k_{D1} + k_{D2}}))) \\
&+ k\,\mathrm{k_{-2}k_{D2}}\Big(\mathrm{k_{-2}^2}(\mathrm{k_D + 2k_{D1}})\mathrm{k_{D2}}\big(\mathrm{k_{D1}k_{D2}} + \mathrm{k_D}(\mathrm{k_{D1} + k_{D2}})\big) \\
&+ \mathrm{k_1^2k_{D1}}\Big(4\mathrm{k_{D1}^2k_{D2}} + \mathrm{k_D^2}(\mathrm{k_{D1} + k_{D2}}) + \mathrm{k_Dk_{D1}}(4\mathrm{k_{D1}} + 7\mathrm{k_{D2}})\Big) \\
&+ \mathrm{k_1k_{-2}}\Big(\mathrm{k_D^2}(\mathrm{k_{D1} + k_{D2}})^2 + 2\mathrm{k_{D1}^2k_{D2}}(\mathrm{k_{D1} + 2k_{D2}}) + \mathrm{k_Dk_{D1}}\big(2\mathrm{k_{D1}^2} + 9\mathrm{k_{D1}k_{D2}} + 5\mathrm{k_{D2}^2}\big)\Big)\Big) \\
&+ \mathrm{c\,k_{-2}}(2k^2(\mathrm{k_D + 2k_{D1}})(\mathrm{k_D} + \mathrm{k_{D1}} + \mathrm{k_{D2}})(\mathrm{k_1k_{D1}} + \mathrm{k_{-2}k_{D2}}) \\
&+ 3\mathrm{k_1k_{-2}k_{D1}k_{D2}}(\mathrm{k_1k_{D1}} + \mathrm{k_{-2}k_{D2}})\big(2\mathrm{k_{D1}k_{D2}} + \mathrm{k_D}(\mathrm{k_{D1} + k_{D2}})\big) \\
&+ k(\mathrm{k_1^2k_{D1}^2}(\mathrm{k_D + 2k_{D1}})(\mathrm{k_D} + \mathrm{k_{D1}} + 2\mathrm{k_{D2}}) \\
&+ \mathrm{k_{-2}^2k_{D2}^2}\Big(\mathrm{k_D^2} + \mathrm{k_D}(4\mathrm{k_{D1}} + \mathrm{k_{D2}}) + 2\mathrm{k_{D1}}(\mathrm{k_{D1}} + 2\mathrm{k_{D2}})\Big) + \mathrm{k_1k_{-2}k_{D1}k_{D2}}(2\mathrm{k_D^2} \\
&+ 4\mathrm{k_{D1}}(\mathrm{k_{D1}} + 3\mathrm{k_{D2}}) + \mathrm{k_D}(11\mathrm{k_{D1}} + 7\mathrm{k_{D2}}))))))\,.
\end{aligned}
\tag{4}
$$

Expressing the flux as $J = K(c_e - c)$, the coefficient K is a positive-definite function of the substrate concentrations and the temperature. It has a strong dependence upon the temperature (*via* the k's and the k_D's) and a significant dependence upon the EC and IC concentrations through Eq. (4).

Part III. Alternative fittings to the experimental data.

Instead of Eq. (4), we now use a simple diffusion-over-a-barrier formula (Eq. (7) of Ref. 2) to fit with the experimental data. In the simple diffusion model[2-7], $K = 1/\int dz[e^{\frac{PMF(z)-\Delta W_0}{RT}}/D(z)] \simeq De^{-(\Delta W_{EC}-\Delta W_0)/RT}$ with the diffusivity D as a fitting parameter. If the simple diffusion formula is valid for the glycerol transport through erythrocytes, then the fitted values of D should be independent of the glycerol concentrations and weakly dependent on the temperatures (~RT, with the absolute temperature T varied from 278.45K to 309.75K in our experiments). The fittings are shown in Figs. S6 to S9. The fitted values of D are tabulated in Table V of the main text. Both the temperature-dependence and the concentration-dependence of the fitted D indicate that the simple diffusion-over-a-barrier model is not valid for glycerol transport through aquaglyceroporins.

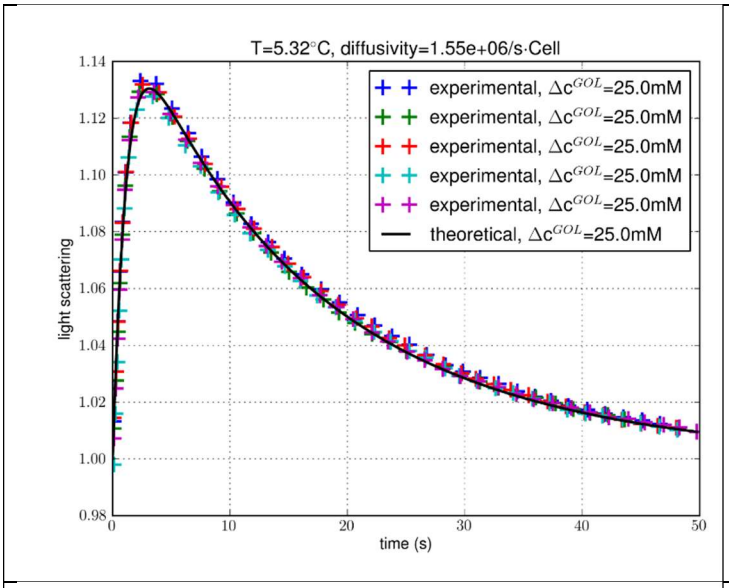

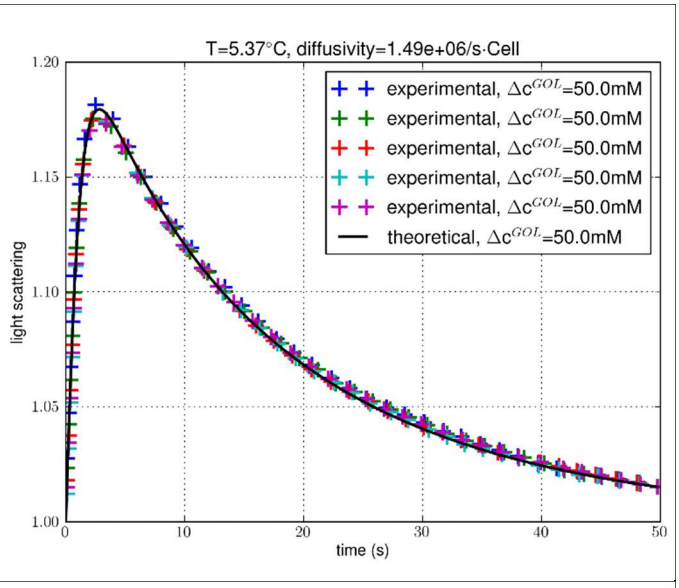

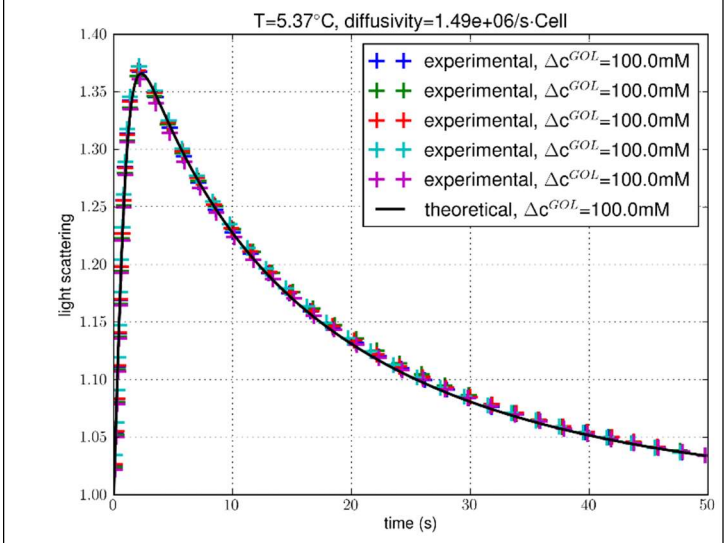

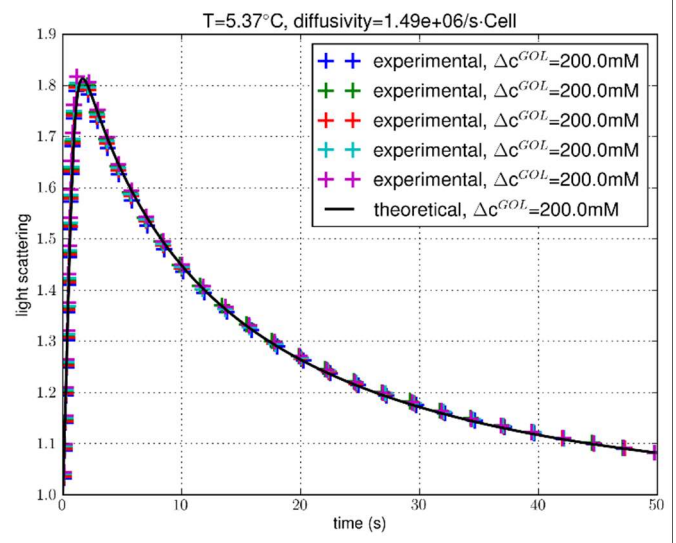

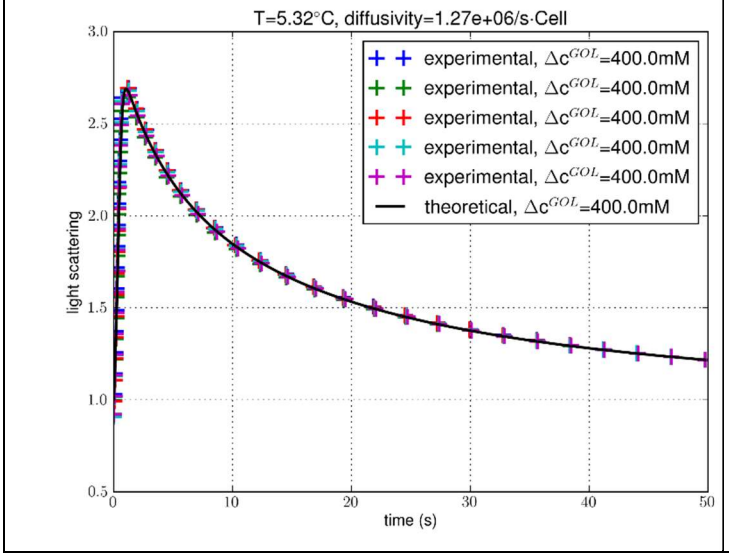

Fig. S6. Experiments at ~5°C of glycerol uptake into human erythrocytes for extracellular glycerol concentration at 25 mM, 50 mM, 100 mM, 200 mM, and 400 mM. The data points (colored crosses) represent normalized intensity of light scattered at 90° immediately after mixing of an erythrocyte suspension in 0.7 ×PBS (containing no glycerol) with an equal volume of 0.7 ×PBS containing $2 \times \Delta c^{GOL}$ glycerol. Five colors represent five experimental repeats under identical conditions. The black solid curve is the predicated time course based on the simple diffusion model with a single fitting parameter diffusivity whose fitted values are shown. The fitting has a p-value less than 10^{-5} in all five sets and a relative error ~5%.

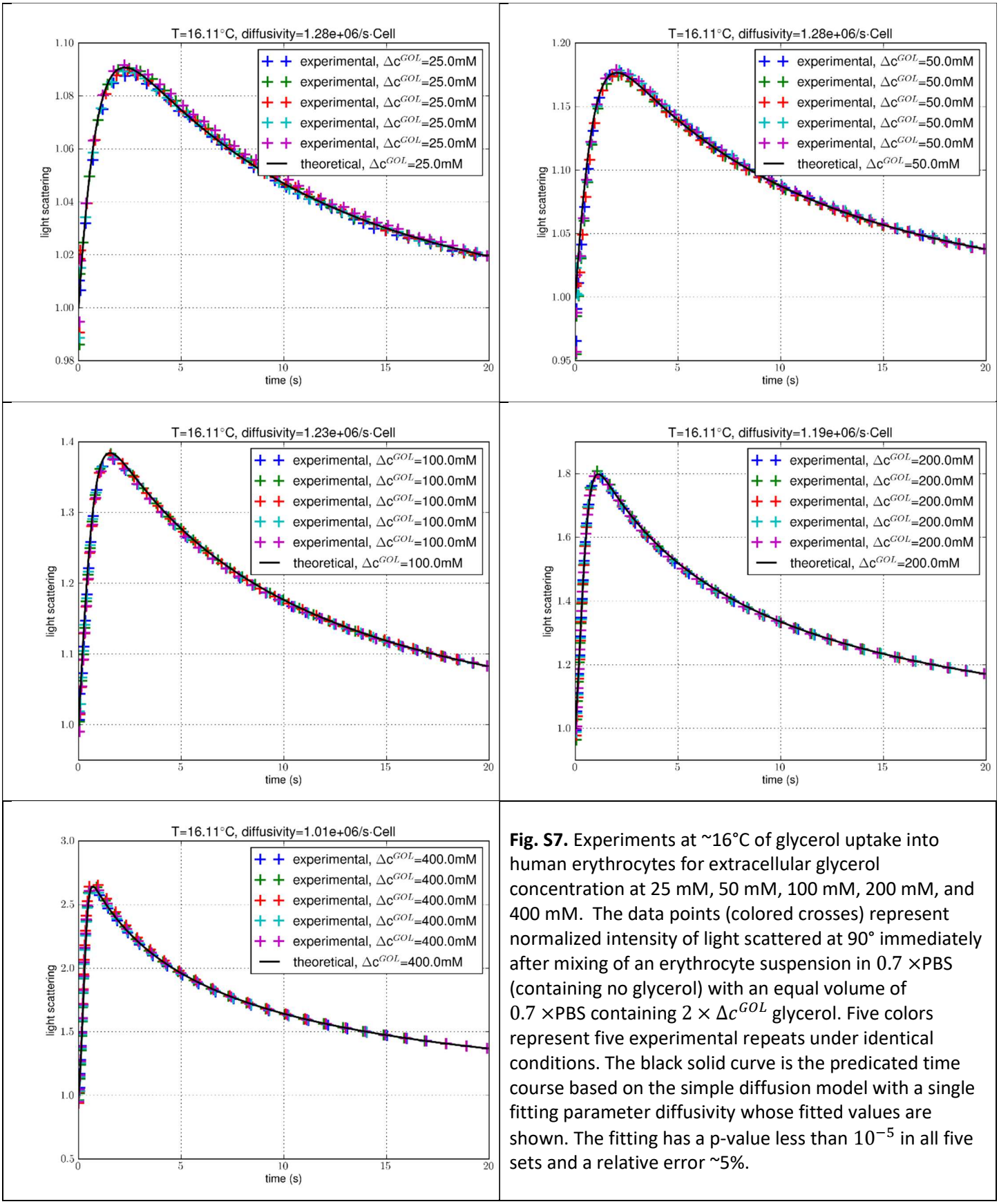

Fig. S7. Experiments at ~16°C of glycerol uptake into human erythrocytes for extracellular glycerol concentration at 25 mM, 50 mM, 100 mM, 200 mM, and 400 mM. The data points (colored crosses) represent normalized intensity of light scattered at 90° immediately after mixing of an erythrocyte suspension in 0.7 ×PBS (containing no glycerol) with an equal volume of 0.7 ×PBS containing $2 \times \Delta c^{GOL}$ glycerol. Five colors represent five experimental repeats under identical conditions. The black solid curve is the predicated time course based on the simple diffusion model with a single fitting parameter diffusivity whose fitted values are shown. The fitting has a p-value less than 10^{-5} in all five sets and a relative error ~5%.

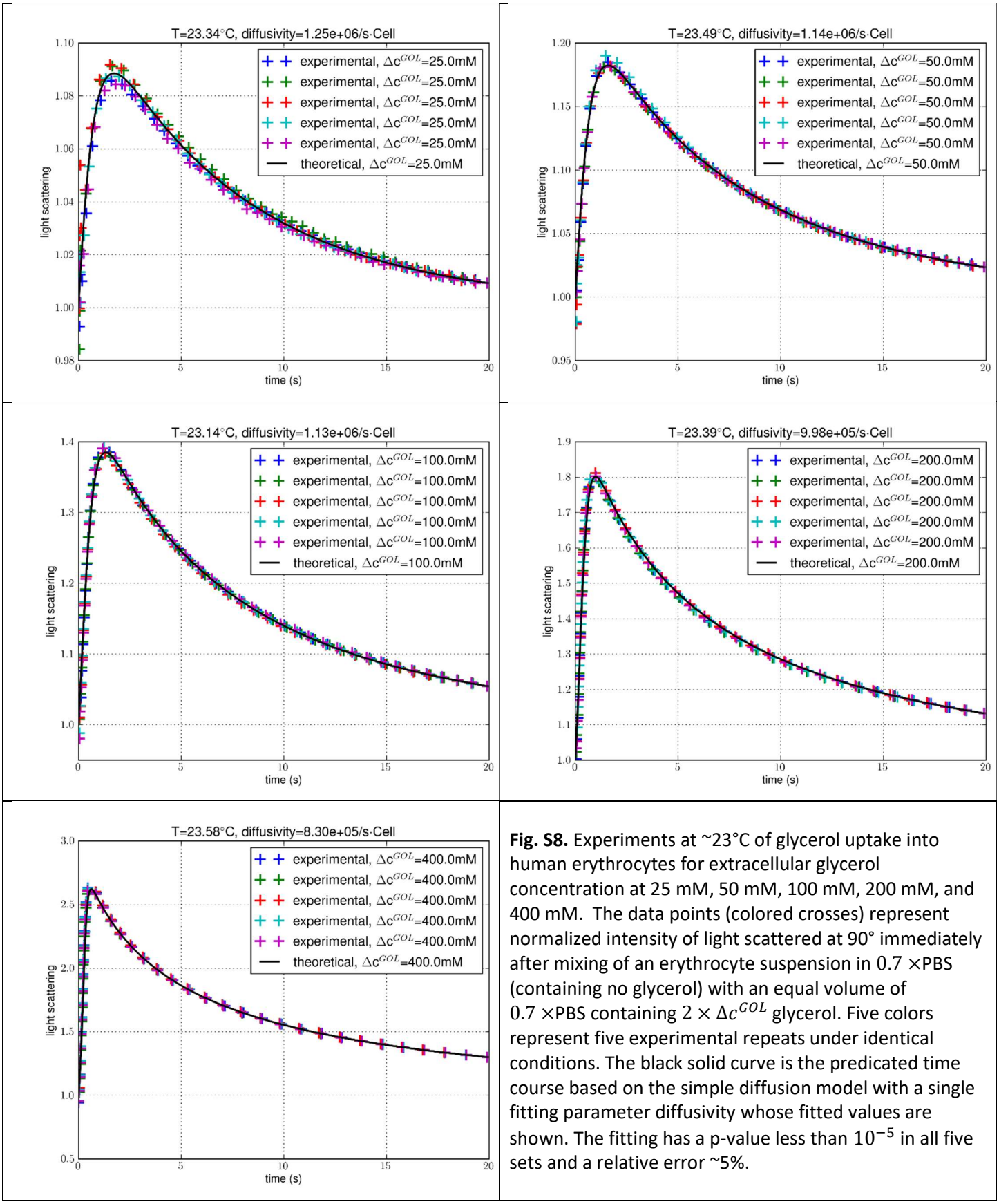

Fig. S8. Experiments at ~23°C of glycerol uptake into human erythrocytes for extracellular glycerol concentration at 25 mM, 50 mM, 100 mM, 200 mM, and 400 mM. The data points (colored crosses) represent normalized intensity of light scattered at 90° immediately after mixing of an erythrocyte suspension in 0.7 ×PBS (containing no glycerol) with an equal volume of 0.7 ×PBS containing $2 \times \Delta c^{GOL}$ glycerol. Five colors represent five experimental repeats under identical conditions. The black solid curve is the predicated time course based on the simple diffusion model with a single fitting parameter diffusivity whose fitted values are shown. The fitting has a p-value less than 10^{-5} in all five sets and a relative error ~5%.

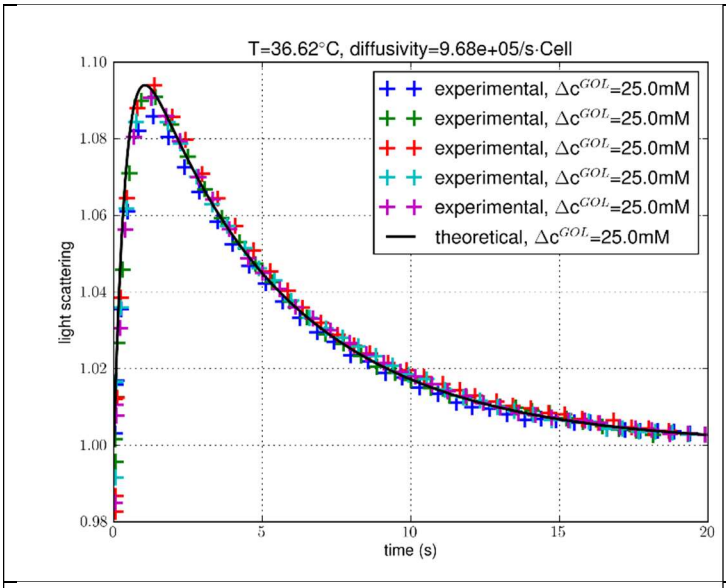

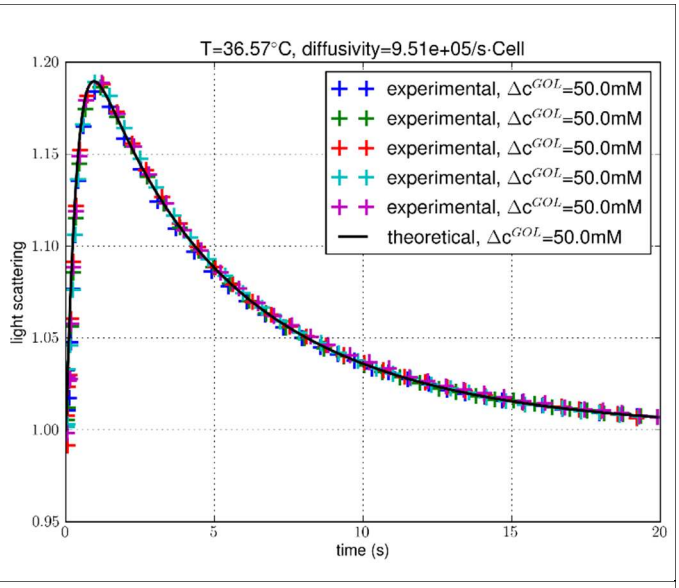

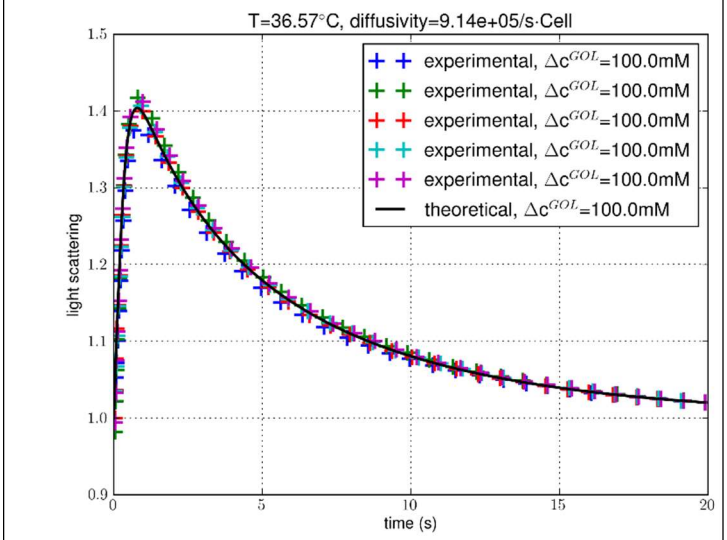

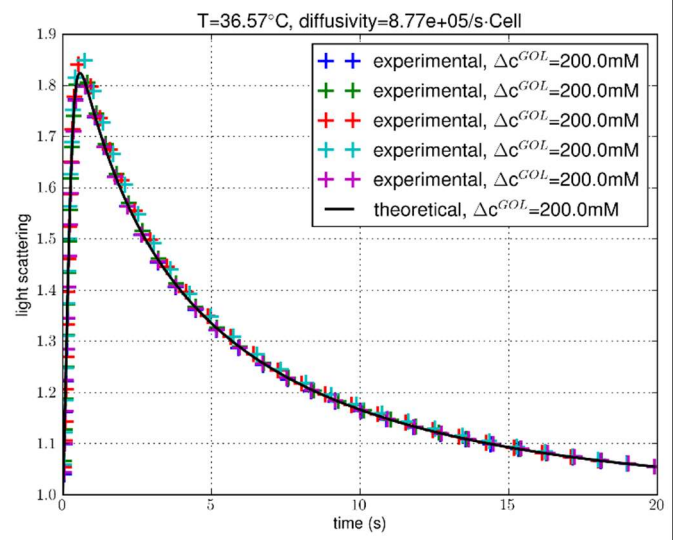

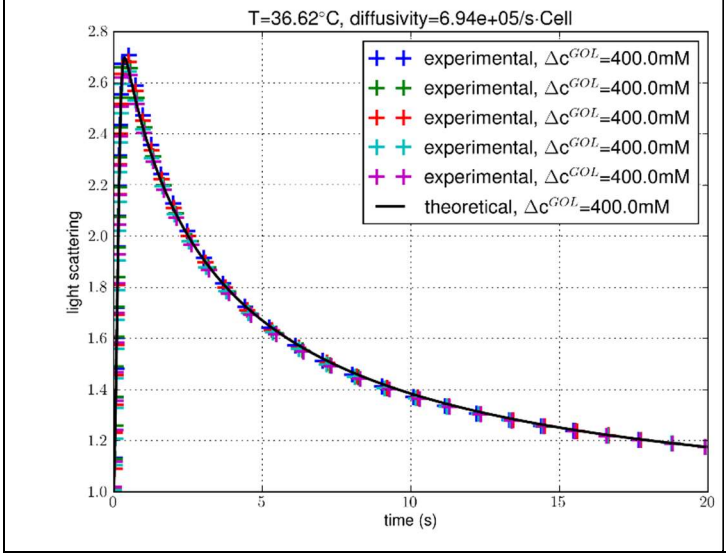

Fig. S9. Experiments at ~37°C of glycerol uptake into human erythrocytes for extracellular glycerol concentration at 25 mM, 50 mM, 100 mM, 200 mM, and 400 mM. The data points (colored crosses) represent normalized intensity of light scattered at 90° immediately after mixing of an erythrocyte suspension in 0.7 ×PBS (containing no glycerol) with an equal volume of 0.7 ×PBS containing $2 \times \Delta c^{GOL}$ glycerol. Five colors represent five experimental repeats under identical conditions. The black solid curve is the predicated time course based on the simple diffusion model with a single fitting parameter diffusivity whose fitted values are shown. The fitting has a p-value less than 10^{-5} in all five sets and a relative error ~5%.

References

1. W. Humphrey, A. Dalke and K. Schulten, *Journal of Molecular Graphics*, 1996, **14**, 33-38.
2. M. Orsi and J. W. Essex, *Soft Matter*, 2010, **6**, 3797-3808.
3. J. M. Diamond and Y. Katz, *The Journal of Membrane Biology*, 1974, **17**, 121-154.
4. S.-J. Marrink and H. J. C. Berendsen, *The Journal of Physical Chemistry*, 1994, **98**, 4155-4168.
5. S. Mitragotri, M. E. Johnson, D. Blankschtein and R. Langer, *Biophys J*, 1999, **77**, 1268-1283.
6. W. T. Coffey, Y. P. Kalmykov, S. V. Titov and B. P. Mulligan, *Phys Rev E Stat Nonlin Soft Matter Phys*, 2006, **73**, 061101.
7. T. X. Xiang and B. D. Anderson, *Advanced drug delivery reviews*, 2006, **58**, 1357-1378.